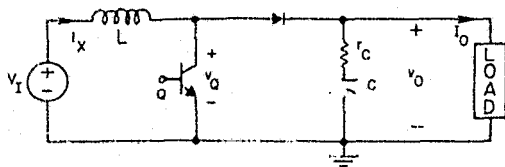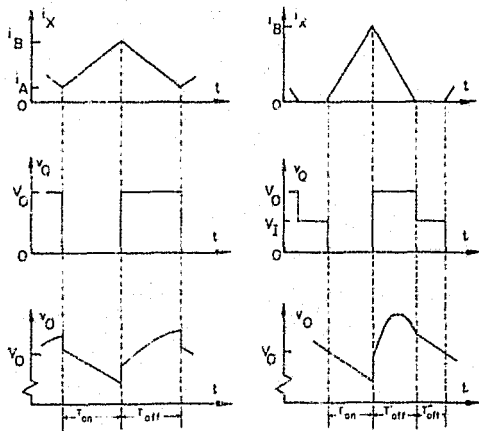# General Disclaimer

One or more of the Following Statements may affect this Document

- This document has been reproduced from the best copy furnished by the organizational source. It is being released in the interest of making available as much information as possible.

- This document may contain data, which exceeds the sheet parameters. It was furnished in this condition by the organizational source and is the best copy available.

- This document may contain tone-on-tone or color graphs, charts and/or pictures, which have been reproduced in black and white.

- This document is paginated as submitted by the original source.

- Portions of this document are not fully legible due to the historical nature of some of the material. However, it is the best reproduction available from the original submission.

Produced by the NASA Center for Aerospace Information (CASI)

STATE-PLANE TRAJECTORIES USED TO OBSERVE AND CONTROL THE BEHAVIOR OF A VOLTAGE STEP-UP DC-TO-DC CONVERTER

William W. Burns, III   Thomas G. Wilson

Department of Electrical Engineering
Duke University, Durham, N. C.

ABSTRACT

State-plane analysis techniques are employed to study the voltage step-up energy-storage dc-to-dc converter. Within this framework, an example converter operating under the influence of a constant on-time and a constant frequency controller is examined. Qualitative insight gained through this approach is used to develop a conceptual free-running control law for the voltage step-up converter which can achieve steady-state operation in one on/off cycle of control. Digital computer simulation data is presented to illustrate and verify the theoretical discussions presented.

INTRODUCTION

As the field of power electronics has evolved and matured, increasingly more attention has been given to analyzing, simulating, and understanding the principles of operation of the highly nonlinear power-processing subnetworks which often are the building blocks of modern power electronics equipment. In recent years, considerable success has been realized in this endeavor. There now are available a variety of mathematical analyses and computer simulation techniques which enable detailed quantitative examinations of particular power inverter and converter configurations [1-12]. In addition to applying such quantitative techniques and approaches, it often is useful to examine complex nonlinear networks in a qualitative manner for the purpose of enhancing a conceptual visualization of the system nonlinearities. It is the nonlinearities which usually are the principal cause of difficulty in analyzing and understanding the system behavior, but, at the same time, they are usually the keystone for successful circuit operation. One such qualitative approach to the study of nonlinear networks and systems which enables a useful visualization of overall system behavior is the phase plane or, more generally, the state-space approach [13].

This paper presents a study of the voltage step-up dc-to-dc energy-storage converter, a highly nonlinear power electronics network, which employs such a state-space approach as a means for revealing considerable qualitative insight into the fundamental behavior of this converter in both steady-state and transient operation. As a demonstration of how this theoretical insight can be used, a new conceptual converter control law is developed which can, in theory, achieve steady-state operation within one "on/off" switching cycle, regardless of the system's initial state or operating conditions.

After introducing the particular dc-to-dc converter configuration which is used throughout the paper to illustrate this approach, a general discussion of converter behavior as it can be characterized in the state plane is presented. Particular attention is given to observing how the system behavior changes when subjected to changes in system parameters or externally imposed operating conditions. This technique is then employed to portray the transient step-load-change response of an example converter functioning under the influence of two commonly used controller configurations, specifically, a constant on-time controller and a constant frequency controller. A third control law is then developed which employs the information contained in the system state trajectories as the basis for determining the transistor switching sequence. Digital computer simulation data are presented to illustrate and verify the theoretical discussions presented.

NORMALIZED CONVERTER AND MODEL

Throughout this paper, the voltage step-up or "boost" dc-to-dc converter is used to illustrate and verify the concepts and techniques discussed. A simplified schematic diagram of this converter is presented in Fig. 1(A) with pertinent characteristic waveforms which depict its operation in the continuous conduction mode, Fig. 1(B), and the discontinous conduction mode, Fig. 1(C). The equivalent series resistance (ESR) of the output capacitor, shown as r_c, has been included in this diagram because it has been found to play an important and sometimes dominant role in converter system behavior [2]. The voltage step-up configuration has been chosen as the example converter for this study because of aggravated stability problems often encountered with this converter, and because it

(A)

(B)   (C)

Fig. 1. (A) Simplified schematic diagram of the
voltage step-up dc-to-dc converter. Character-
istic waveforms for (B) operation in the contin-
uous conduction mode, and (C) operation in the
discontinuous conduction mode. Example circuit
values are: $L=0.05$ mH, $C=350$ µF, $r_c=0.05\Omega$,
$V_{0,rated}=28.0V$, $V_{I,rated}=21.0V$, and $I_{0,rated}=5.0A$.

presents greater analytical difficulties than some
of the other commonly used inductor-energy-storage
configurations.

For the purpose of generality and to facilitate
relative comparisons, the converter of Fig. 1 has
been normalized as shown in Fig. 2. Normalization
factors are chosen so that the normalized rated
average output voltage is unity, the normalized
rated output current is unity, and a normalized
time of 2π corresponds to the undamped natural
period of the inductor-capacitor combination in the
unnormalized converter power stage. All data
presented in this paper are in normalized form, and
the symbols introduced in Fig. 2 with the subscripts
N are used to distinguish normalized variables and
parameters from their unnormalized counterparts.

To be amenable to mathematical analysis, any
physical system must be modeled in such a way as to
capture those aspects of the system behavior which
are essential to its operation and which, addi-
tionally, focus attention on items of particular
interest. Two such abstractions of the physical
voltage step-up converter are presented in Figs.
1(A) and 2. A third model is presented in Fig. 3
where Fig. 3(A) shows the equivalent circuit when
the transistor switch is "on" or closed, and Fig.
3(B) when the transistor switch is "off" or open.
The model portrayed in Fig. 3 has a relatively
simple mathematical respresentation but, at the
same time, retains the essential principles of
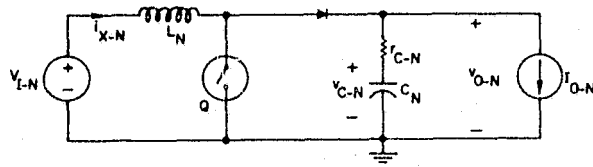
Fig. 2. Normalized representation of power stage
with normalization factors $V_{ref}=V_{0,rated}$, $I_{ref}=I_{0,rated}$, and $T_{ref}=\sqrt{LC}$. Normalized circuit para-
meters and variables in terms of original network
values are:

$$L_N=\frac{I_{ref}}{V_{ref}T_{ref}}L \qquad V_{I-N}=\frac{V_I}{V_{ref}} \qquad V_{0-N}=\frac{V_0}{V_{ref}}$$

$$C_N=\frac{V_{ref}}{I_{ref}T_{ref}}C \qquad i_{X-N}=\frac{i_X}{I_{ref}} \qquad I_{0-N}=\frac{I_0}{I_{ref}}$$

$$r_{C-N}=\frac{I_{ref}}{V_{ref}}r_C \qquad V_{C-N}=\frac{V_C}{V_{ref}} \qquad t_N=\frac{t}{T_{ref}}$$
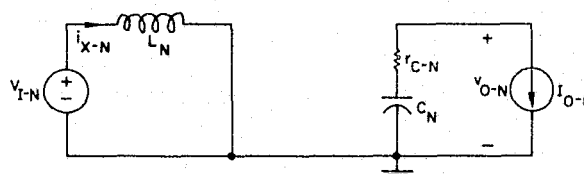
(A)
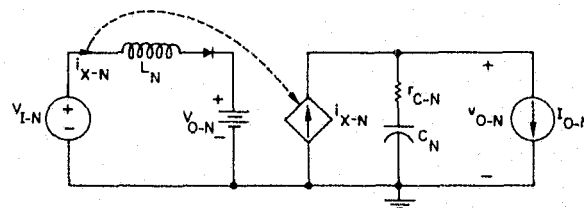
(B)

Fig. 3. Converter model during (A) transistor
on-time, and (B) transistor off-time.

operation of the actual physical system. Thus, for
the sake of convenience in generating desired data,
this simplified model is used. It should be noted,
however, that the validity of the theoretical treat-
ment presented in this paper is not dependent on the
particular simplified converter model depicted in
Fig. 3. The same arguments and equivalent data can
be generated for converter models of considerably
greater complexity.

For the particular model presented in Fig. 3,
the power transistor is assumed to be an ideal
switch, and likewise the diode is assumed to be
ideal. The output voltage is assumed to be suf-
ficiently well regulated that the load can be
represented as a constant current sink. During
the transistor off-time, it is assumed that the
output voltage ripple is not great enough to
influence the shape of the inductor current wave-
form so that the voltage across the transistor
during T_{off-N} is assumed to be constant and equal
to the average output voltage V_{0-N}. The resul-
tant inductor current i_{X-N} is then used, in con-

junction with the output current I_{0-N} , to compute the capacitor current and subsequently the capacitor voltage v_{C-N} . This model yields solutions to the system state equations which are algebraic functions of time and thus are easy to visualize. More exact models yield solutions which, although transcendental in nature, are equally amenable to this state-plane treatment but are less readily visualized without the aid of detailed computation.

CONVERTER BEHAVIOR IN THE STATE PLANE

The converter system state variables employed in this study are the normalized reactor current i_{X-N} and the normalized capacitor voltage v_{C-N} . The behavior of the converter can be represented mathematically by means of a sequence of pairs of differential equations which can be solved explicitly to yield time-domain solutions for the state of the system. If the independent variable, normalized time, is eliminated in the solutions $i_{X-N}(t_N)$ and $v_{C-N}(t_N)$, a sequence of equations of the form $v_{C-N} = g(i_{X-N})$ results, where now time is an implicit parameter. These implicit equations, when plotted in the state plane of i_{X-N} versus v_{C-N} define what is called the solution curve, or the system state trajectory. Those portions of a solution curve which result when the transistor is on are referred to as on-time trajectories, and those portions corresponding to the transistor being off are referred to as off-time trajectories. The complete transient response of a converter thus can be portrayed in the state plane as a sequence of connected on-time and off-time trajectories. Normal steady-state operation of a converter is indicated by a closed curve in the state plane consisting of a single on-time trajectory and a single off-time trajectory.

A typical family of on-time and family of off-time trajectories for a particular voltage step-up dc-to-dc converter, whose equations will be derived subsequently, are presented in Fig. 4. Each trajectory corresponds to a different pair of initial conditions or initial state of the system. The family of off-time trajectories, whose initial states have been arbitrarily selected as uniformly spaced points along the translated ordinate axis, are shown as solid lines. Paths, such as these are the ones which the system state must follow whenever the transistor is turned off. Similarly, the on-time trajectories, shown as broken lines, are the paths which the state must follow during the time that the transistor is turned on. As indicated previously, time is an implicit parameter in these state trajectories and, as time increases, the system state moves in the direction indicated by the arrow heads; i.e., decreasing reactor current and peaking capacitor voltage for the off-time trajectories, and increasing reactor current and decreasing capacitor voltage for on-time trajectories. Any converter solution curve, or solution trajectory, is made up of a sequence of such off-time segments and on-time segments.

When employing the model portrayed in Fig. 3, these solution curves can be found to be parabolas for the off-time trajectories and straight lines for the on-time trajectories as derived below. From Fig.
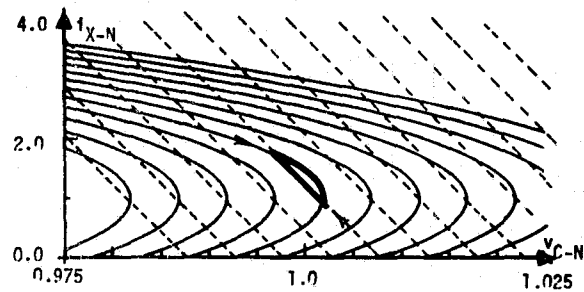
Fig. 4.   Families of on-time trajectories (broken lines) and off-time trajectories (solid lines) in the state plane of i_{X-N} vs. v_{C-N} corresponding to different initial states for the converter shown in Fig. 2 with $V_{I-N}=0.75$, and $I_{0-N}=1.0$. Highlighted closed curve is the steady-state solution trajectory corresponding to nominal rated conditions used as a reference in subsequent figures.

3, one can derive the corresponding sequence of state equations and subsequently the explicit time-domain solutions. Calling t_N^0 the arbitrary initial time and $i_{X-N}(t_N^0)$ and $v_{C-N}(t_N^0)$ the arbitrary initial state variables of the converter, the time-domain solution of the network in Fig. 3(A) for the time interval T_{on-N} that the switch is closed is for

$$t_N^0 \leqslant t_N < t_N^0 + T_{on-N}$$

$$i_{X-N} = \frac{V_{I-N}}{L_N} t_N + i_{X-N}(t_N^0)$$

$$v_{C-N} = - \frac{I_{0-N}}{C_N} t_N + v_{C-n}(t_N^0) \tag{1}$$

Similarly, for that portion of the transistor off-time period T'_{off-N} when the inductor current i_{X-N} is greater than zero in Fig. 3(B), the solutions for the two system state variables for $t_N^0 < t_N < t_N^0 + T'_{off-N}$ are

$$i_{X-N} = - \frac{V_{0-N}-V_{I-N}}{L_N} t_N + i_{X-N}(t_N^0)$$

$$v_{C-N} = - \frac{V_{0-N}-V_{I-N}}{2L_N C_N} t_N^2 + \frac{i_{X-N}(t_N^0)-I_{0-N}}{C_N} t_N + v_{C-N}(t_N^0) \tag{2}$$

For that portion of the transistor off-time period T''_{off-N} when the inductor current i_{X-N} is equal to zero in Fig. 3(B), the solutions for the two system state variables for $t_N^0 < t_N < t_N^0 + T''_{off-N}$ are

$$i_{X-N} = 0$$

$$v_{C-N} = - \frac{I_{0-N}}{C_N} t_N + v_{C-N}(t_N^0) \tag{3}$$

The independent variable t_N can be eliminated in each pair of solutions to yield the following sequence of equations which defines the system state trajectory during each of the three possible time intervals.

$$v_{C-N} = - \frac{L_N I_{0-N}}{C_N V_{I-N}} i_{X-N} + K_1 \qquad (4)$$

$$v_{C-N} = - \frac{L_N}{2C_N(V_{0-N}-V_{I-N})} (i_{X-N}^2 - 2I_{0-N}i_{X-N}) + K_2 \quad (5)$$

$$i_{X-N} = 0 \qquad (6)$$

K_1 and K_2 are constants which are determined from the circuit component values, the converter operating conditions, and the particular initial states. Thus, for the converter model chosen, the system on-time trajectories are defined by (4) which gives the family of straight lines of Fig. 4. Likewise, the portions of the off-time trajectories which occur during T'_{off-N} are defined by (5) which gives the family of parabolas of Fig. 4. The portions of off-time trajectories corresponding to T''_{off-N} are defined by (6) and are simply segments of the v_{C-N} axis with the direction of movement of the state when on this axis being toward the origin of the plane. The trajectories defined by (6) occur during the zero-current dwell time of the system when operating in the discontinuous conduction mode.

The trajectories plotted in Fig. 4 are shown only in a localized region of the state plane with a voltage range of ±2.5% of the rated output voltage and a current range of 0 to 4 times the rated output current. This particular region of the plane is displayed because it includes the steady-state trajectory of the example converter operating with the input voltage and output current specified in Fig. 1. This steady-state trajectory is highlighted with bold lines near the center of Fig. 4 and is seen to be comprised of segments of one off-time trajectory and one on-time trajectory. The particular closed trajectory illustrated here corresponds to steady-state operation in the continuous conduction mode under rated conditions, and it is used as a reference in subsequent illustrative data. Examples of discontinuous conduction trajectories, consisting of three distinct segements as described in the preceding paragraph, are presented later in the paper.

Given any initial state within this plane, the transient trajectory which the system state follows in attempting to reach a steady-state condition is determined by the sequence of power switch closings and openings as established by the converter controller. That is, as long as the transistor switch is off, the system state must follow the particular off-time trajectory which passes through the state at the instant the switch is turned off. At the instant the switch is turned on, the state must begin to follow the particular on-time trajectory which passes through the final state of the preceding off-time trajectory. In this manner, the state of the system alternately follows off-time and on-time trajectories around the state
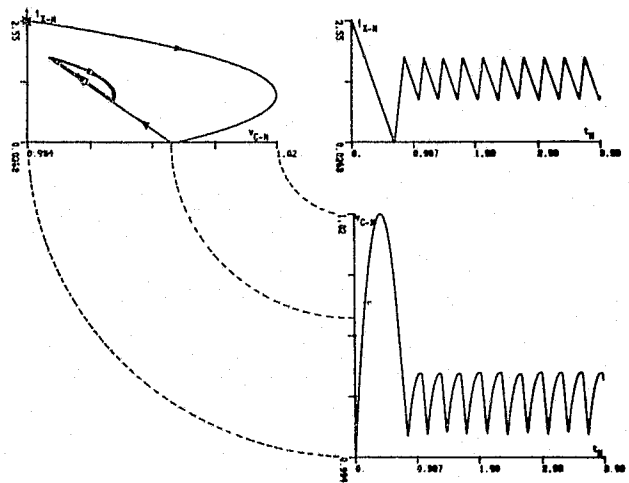
Fig. 5. Illustration of relationship between state-plane solution trajectory (upper left) and state-variable time waveshapes (right) for converter of Fig. 1. The solution trajectory is composed of segments from the two families displayed in Fig. 4.

plane, and eventually, if the converter system is functioning properly, converges to a closed steady-state trajectory. Such a sequence of trajectories is illustrated in Fig. 5.

From an initial state of (2.55, 0.994) marked with an X in the i_{X-N} vs. v_{C-N} plane, the off-time trajectory which passes through this initial state is followed as time increases until the transistor is switched on at some time by the action of the converter's controller. The on-time trajectory which passes through the final off-time state is then followed until the transistor is again turned off by the controller. In the example illustrated here, the solution trajectory converges to the closed two-segment curve shown in the left center portion of the plane. The off-time and on-time trajectories traversed in this figure are members of the families of off-time and on-time trajectories displayed in Fig. 4, and the steady-state trajectory of Fig. 5 is the same as that highlighted with bold lines in Fig. 4. The relationship between the state trajectories and the more familiar current and voltage vs. time waveforms is also seen in Fig. 5.

As discussed and derived in preceding paragraphs of this section, the shapes of the system state trajectories are well defined and known functions of the network parameters such as the system inductance and capacitance and of the externally imposed operating conditions such as the input voltage and the output current. Thus, a change in any of these parameters or, more likely, a change in operating conditions, causes the shapes of these trajectories to change accordingly. For example, Fig. 6(A) illustrates how, starting from common initial states indicated by the black squares, the shapes of the off-time and on-time trajectories change when converter output current increases from no load to 200% of full load. The initial state for the off-time trajectories in this illustration corresponds to the
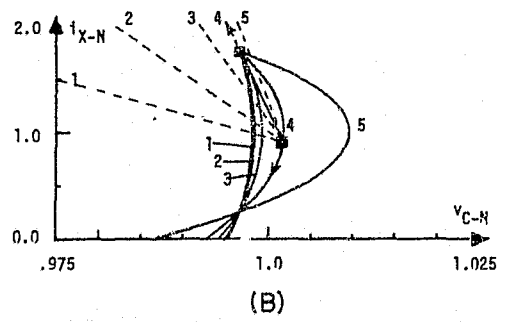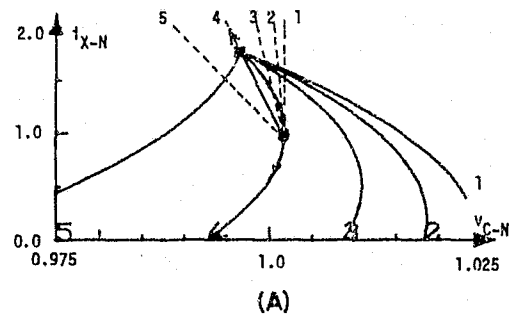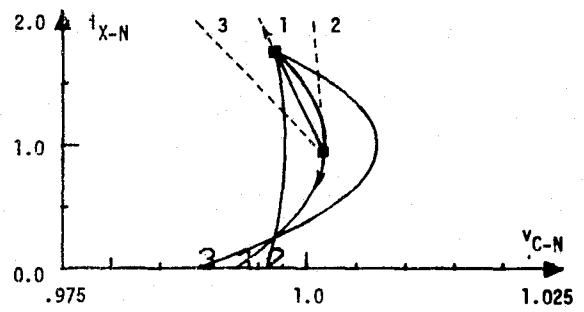
(A)

(B)

Fig. 6. Change in shape of on-time trajectories
  (broken lines) and off-time trajectories (solid
  lines) for
  (A) V_{I-N} constant at 0.75 and I_{0-N}= 1) 0.0,
      2) 0.2, 3) 0.5, 4) 1.0, and 5) 2.0.
  (B) I_{0-N} constant at 1.0 and V_{I-N}= 1) 0.1,
      2) 0.25, 3) 0.5, 4) 0.75, and 5) 0.9.

instant in the steady-state cycle of Fig. 4 when
the transistor switch turns off. Likewise, the
initial state for the five on-time trajectories is
chosen as the switch-on instant in the same refer-
ence steady-state cycle. This reference steady-
state solution trajectory can also be seen in Fig.
6(A) as the solid closed curve made up of segments
corresponding to the rated output current and in-
dicated on the figure as load condition number four.
Note that the range of the reactor current in this
figure is 0 to 2 units rather than 0 to 4 units as
in Fig. 4 so that the steady-state trajectory
appears enlongated in the vertical direction. A
similar example of how the shapes of the trajectory
segments change for various values of input voltage
is presented in Fig. 6(B) where the same initial
states are used, and the reference steady-state tra-
jectory of Fig. 4 is again displayed as the closed
curve consisting of segments corresponding to input-
voltage condition number four.

     As mentioned previously, the shapes of the
system state trajectories are also dependent on the
values of the system parameters. Of particular
interest to converter designers is the effect of
changing the value of the energy-storage inductance.
The value of inductance often is chosen to insure
converter operation in either the continuous or the
discontinuous conduction mode over a specified range
of operating conditions. Fig. 7 presents the off-
time trajectories and the on-time trajectories for
three different values of inductance in converters

Fig. 7. Changes in shape of on-time trajectories
  (broken lines) and off-time trajectories (solid
  lines) for V_{I-N}=0.75, I_{0-N}=1.0, and decreasing
  inductance L_N= 3) 0.095, 1) 0.067, and 2) 0.03.

which are otherwise identical and which are running
under the same set of operating conditions. The
trajectories labeled 1 correspond to the value of
inductance which has been used as the reference value
in previous illustrations. One can see the now
familiar reference steady-state trajectory near the
center of the figure. As one might expect, the
steady-state trajectories which exist for the other
two illustrative values of inductance are quite
different. All three of these trajectories are shown
in Fig. 8 for the same values of input supply volt-
age, average output voltage, and average load cur-
rent. For large values of inductance, steady-state
operation is in the continuous conduction mode, Figs.
8(A) and (B). With sufficiently small values of
inductance, as illustrated in Fig. 8(C), the steady-
state operation of the converter is in the dis-
continuous conduction mode as can be seen by the
solution trajectory incorporating a portion of the
abscissa corresponding to zero reactor current dur-
ing a portion of the transistor off-time. Thus,
one can see that these three converters, which are
identical except for the values of inductance, ac-
complish the same power processing task but in
markedly different manners which are consistent with
the requirements of the individual shapes of their
respective on-time and off-time trajectories.

          CONVERTER CONTROL FUNCTIONS PORTRAYED
                  IN THE STATE PLANE

     As discussed in an earlier section, the partic-
ular transient trajectory that the system state
follows in attempting to reach a steady-state con-
dition is entirely dependent on the particular
control function applied to the converter power
switch. In this section, the analytical framework
described above is employed to examine two commonly
used converter controllers.

Constant On-Time Controller

     A constant on-time or pulse frequency modulation
controller is depicted conceptually in Fig. 9. This
controller monitors the output voltage v_{0-N} of the
converter power stage and compares it to a constant
reference voltage v_{R-N} . When the output voltage is
less than the reference voltage, two monostable
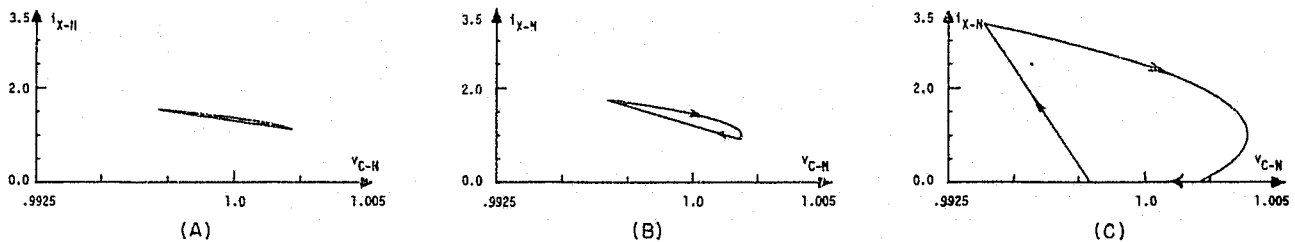multivibrators are activated; one produces a pulse

Fig. 8. Steady-state trajectories for the converter of Fig. 2 operating at $V_{I-N}=0.75$, $I_{0-N}=1.0$, and successively smaller values of inductance: (A) $L_N=0.095$, (B) $L_N=0.067$, and (C) $L_N=0.03$.

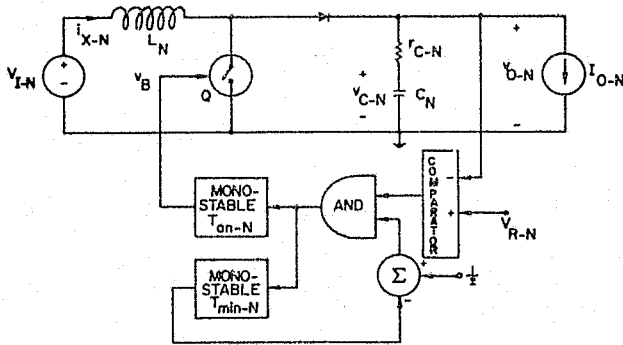
Fig. 9. Conceptual diagram of a constant on-time controller system. Example values are:
$V_{R-N} = 1.0$, $T_{on-N} = 0.075$, and $T_{min-N} = 0.25$.

(A)

(B)

Fig. 10. (A) Off-time trajectories, and (B) on-time trajectories plotted in the i_{X-N} vs. v_{0-N} plane for the controller-converter system of Fig. 9 with $V_{I-N}=0.75$, and $I_{0-N}=1.0$.

of width T_{on-N}, equal to the constant on-time specified, and the other a pulse of width equal to the on-time plus a specified minimum off-time which yeilds, in effect, a minium switching period equal to T_{min-N}. The output of the upper monostable multivibrator turns switch Q on for the specified T_{on-N}, whereas the output from the lower multivibrator is subtracted from a constant value such that it gives a negative input to the AND gate. This insures that the upper multivibrator cannot be activated again until after waiting a minimum time T_{min-N} even if the output voltage never exceeds the reference. If the output voltage is greater than the reference, the upper input to the AND gate is negative and the turn-on signal cannot be activated.

Fig. 10 presents selected families of off-time trajectories and on-time trajectories which illustrate certain aspects of this particular control technique. In this case, notice that the abscissas for these plots are v_{0-N} rather than v_{C-N}. The output voltage v_{0-N} can be determined from a knowledge of v_{C-N} and has replaced v_{C-N} in this figure because it is the signal normally monitored in actual circuit implementations, not the ideal capacitor voltage which is very difficult to measure experimentally. The two heavy vertical lines at $v_{0-N} = V_{R-N}$ are the switch-on lines.

On observing Fig. 10(A), one can see two illustrative off-time trajectories which never intersect the vertical switching line. If an initial turn-off state of the system is such that one of these off-time trajectories is followed, the desired reference switch-on condition cannot be achieved and the back-up minimum off-time criteria must issue the transis-

tor turn-on signal. One can also see from Fig. 10 (A) that, in order to achieve the desired reference-level turn-on operation with this controller, the output voltage must peak during the transistor off-time and fall back to cross the vertical switching line from right to left. Thus, if the location of the desired steady-state trajectory for a given set of operating conditions falls within a region of the state plane where the off-time trajectories do not peak, see for example Fig. 8(A), the converter cannot operate in the desired mode and unstable operation results.

Fig. 10(B) illustrates a particular set of on-time trajectories. The restricted lengths of the solid-line portions of these trajectories are due to the fixed parameter T_{on-N}. On-time trajectories can be observed anywhere in the state plane left of the vertical switching line, but the on-time trajectories which correspond to the desired reference-level turn-on condition of operation always begin on the verti-
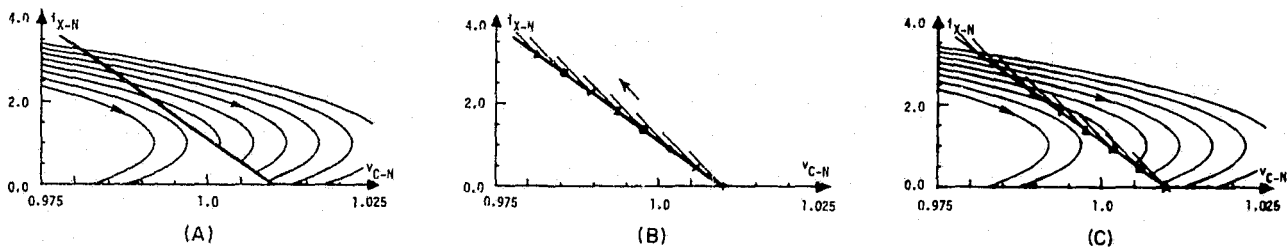
Fig. 11. (A) Off-time trajectories and (B) on-time trajectories of Fig. 10 mapped into the i_{X-N} vs. v_{C-N} plane. (C) Superposition of (A) and (B).

cal switching line and display an initial jump due to the capacitor ESR voltage drop. These jumps in output voltage at the instant the transistor turns on are indicated by the broken-line portions of the trajectories in Fig. 10(B).

These same off-time and on-time trajectories are mapped into the i_{X-N} vs. v_{C-N} plane in Fig. 11 where the vertical switching line is now seen to be slanted. The slope of this line is a function of the capacitor ESR and, if ESR is neglected, the switching line is vertical. Thus, one effect of the capacitor ESR on converter performance with this type of controller is made evident; i.e., more off-time trajectories can cross the switching line when the output capacitor has larger ESR, thus enabling this particular control technique to accommodate a wider range of operating conditions than it can with a smaller ESR. Near the center of Fig. 11(C) one can see the same familiar closed steady-state trajectory which has served as a reference condition throughout this paper.

Example transient trajectories and corresponding time waveshapes for the voltage step-up converter operating under the influence of this type of controller are presented in Figs. 12 and 13. These data were generated through the IBM Continuous System Modeling Program (CSMP) and were plotted through an X-Y plotter interfaced to the computer. The plot routines automatically scaled the data to completely fill the plot space, thus accounting for the sometimes unusual scaling. A common initial state was chosen for these and all succeeding simulation runs to provide a basis for comparison. The particular initial state chosen is the steady-state switch-off state of the reference steady-state trajectory which has been used throughout this presentation.

Fig. 12 illustrates the response of the controller-converter combination just discussed for a decrease in load current from 100% to 20% of the rated output current. The system initially follows an off-time trajectory which reaches the $i_{X-N} = 0$ axis, and the capacitor voltage continues to fall until the switch-on line is reached. A constant on-time trajectory follows and the system is seen to be in steady state in the discontinuous conduction mode of operation. A normalized voltage of 1.0 units is indicated by the tick mark which is above the v_{C-N} axis, and one can see that with this lighter load, the average capacitor voltage and thus the average output voltage is greater than 1.0. Fig. 13 illustrates the transient response of the same converter
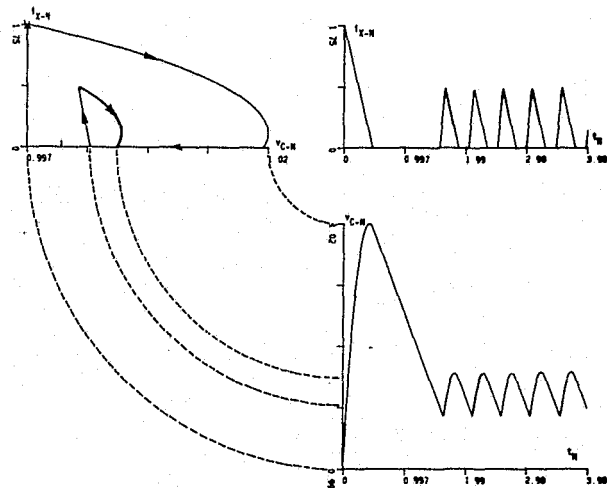

Fig. 12. CSMP generated response of the controller-converter system of Fig. 9 with $V_{I-N}=0.75$ for a step decrease in I_{O-N} from 1.0 to 0.2.
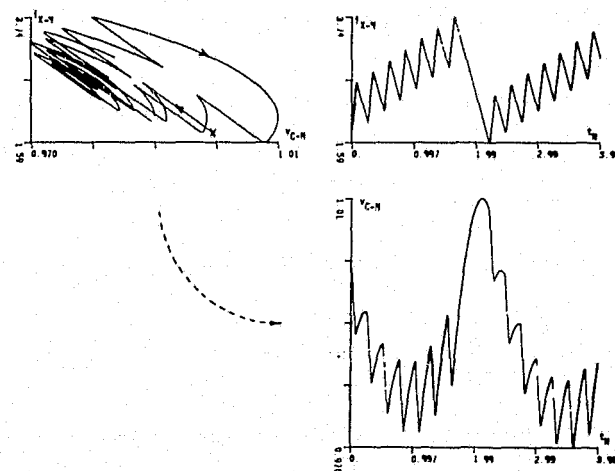

Fig. 13. CSMP generated response of the controller-converter system of Fig. 9 with $V_{I-N} = 0.75$ for a step increase in I_{O-N} from 1.0 to 2.0.

configuration operating under the influence of the same controller, but for an increase in load from 100% to 200% of the rated output current. This heavier load condition changes the shapes of the off-time and on-time trajectories in such a way that the region of the state plane around the desired average voltage and the required average reactor current does not contain peaking off-time trajecto-
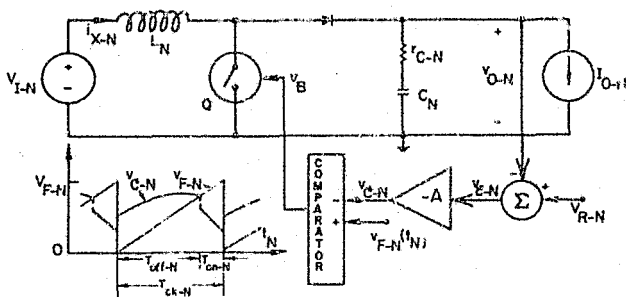
Fig. 14. Conceptual diagram of a constant frequency coincidence detector controller system. Example values are: $V_{R-N}=0.73$, $V_{F-N}=0.035$, $T_{ck-N}=0.30$, and $A=0.1$.

ries. Thus, the converter system is unstable under this load condition and a tendency toward a sub-switching-frequency mode of operation is seen in Fig. 13.

Constant Frequency Controller

A second control technique which is often used with dc-to-dc converters is the constant frequency coincidence detector illustrated conceptually in Fig. 14. In this case, the transistor switch is turned on when the constant frequency sawtooth function $v_{F-N}(t_N)$ is coincident with the analog control signal v_{C-N}. Figs. 15 and 16 illustrate the transient trajectories for the same converter configuration under the same load-change conditions as illustrated in Figs. 12 and 13 but operating under the influence of this constant frequency controller. For the case of the decrease in load current, one can see that the state trajectory is beginning to converge to a steady-state trajectory in the discontinuous conduction mode, but that after 4 units of normalized time, steady-state operation still has not been achieved. For the second case, that of an increase in load current, one again observes the system instability which is not uncommon in the voltage step-up configuration operating under heavy load conditons.

CONCEPTUAL DEVELOPMENT OF A FREE-RUNNING CONTROLLER

A study of the shapes of the system off-time trajectories and on-time trajectories and the manner in which they change for various changes in system parameters and operating conditions has led to considerable insight into the fundamental elements of control required for this type of energy storage dc-to-dc converter. One example of how this insight can be used is illustrated in Fig. 17. This figure again displays off-time and on-time trajectories in the state plane, but in these graphs the plane has been portioned into two regions, with the off-time trajectories being confined to the upper right-hand region and the on-time trajectories to the lower left. The boundary between the regions consists of segments of a particular off-time trajectory and a particular on-time trajectory which are shown as bold lines in each figure. These particular trajectories are chosen to construct the boundary line because they also include the steady-state off-time
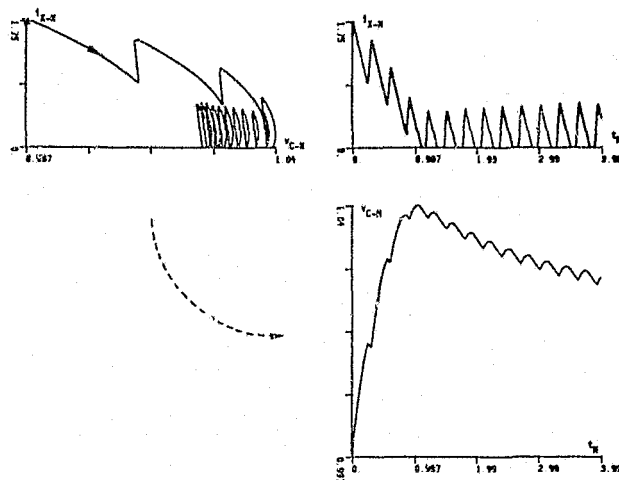

Fig. 15. CSMP generated response of the controller-converter system of Fig. 14 for a step decrease in I_{0-N} from 1.0 to 0.2.
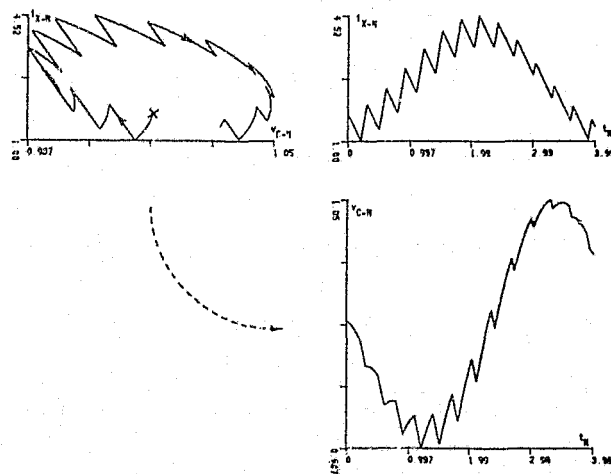

Fig. 16. CSMP generated response of the controller-converter system of Fig. 14 for a step increase in I_{0-N} from 1.0 to 2.0.

and on-time trajectory segments for the given set of operating conditions. The actual steady-state trajectory for each of the three cases is seen as the closed curve at the intersection of the two segments that make up the boundary line in each figure. The steady-state trajectory shown in Fig. 17(B) is the same steady-state trajectory that has been used throughout as the reference case.

The information contained in these figures can be used to determine when to turn the transistor on and off in order to achieve steady-state operation in one on/off cycle of control, regardless of the system's initial state or operating conditions. For example, if the initial state of the system is in the region of the plane below the boundary line, and if the control law is such that the transistor is on when in this region, the system state must follow the corresponding on-time trajectory up-
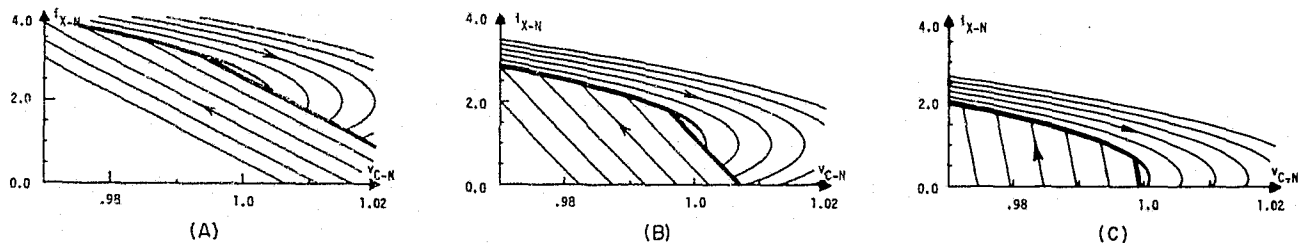
Fig. 17. Off-time and on-time trajectories for the converter configuration of Fig. 2 with $V_{I-N}=0.75$ and $I_{O-N}=$ (A) 2.0, (B) 1.0, and (C) 0.2. Bold lines separate the on-time region from the off-time region of the state plane.

ward and to the left toward the bold boundary line. If, in addition, the controller is such that it uses this boundary as a switch-off line, the transistor turns off at the instant the state reaches this boundary and the off-time trajectory which is then followed coincides with the boundary line. If the controller then uses the on-time segment of the boundary line as a switch-on line, the system state will continue to move around the steady-state trajectory shown adjacent to the switching lines. Likewise, if the control law is such that the transistor is off whenever the system state is above the boundary line, a state in this upper region initially follows an off-time trajectory until the switch-on boundary line is reached, at which time the transistor switches on and the on-time trajectory coinciding with the boundary line is then followed. Thus, one can see that if these boundaries are used as switching lines, the system steady-state trajectory can be attained in one cycle of control; i.e., with one on-time and one off-time, or vice versa, depending on which region of the plane contains the initial state.

After this single initial on/off transient cycle, the converter continues to operate around the steady-state trajectory at a constant frequency. The precise frequency desired is specified through a time parameter that appears in the expressions for K_1 and K_2 of equations (4) and (5), respectively. By means of a static analysis [14], this parameter together with the circuit component values and operating conditions can be used to determine a point on the steady-state trajectory for the given operating conditions. The particular off-time and on-time trajectories which include this point are chosen as the switching lines described above. The system is thus free-running, in the sense that no timing elements are involved, but at the same time operates at a constant frequency in steady-state over the whole range of operating conditions. In both the transient cycle and in steady state, the transistor switching occurs when the system state trajectory intersects well-defined and known switching lines which correspond to a given converter configuration and externally imposed operating conditions.

Fig. 18 presents a conceptual picture of this free-running control process. Four pieces of information are required by the controller to accomplish the decision making process described above. They are v_{I-N}, i_{O-N}, i_{X-N}, and v_{C-N}. The
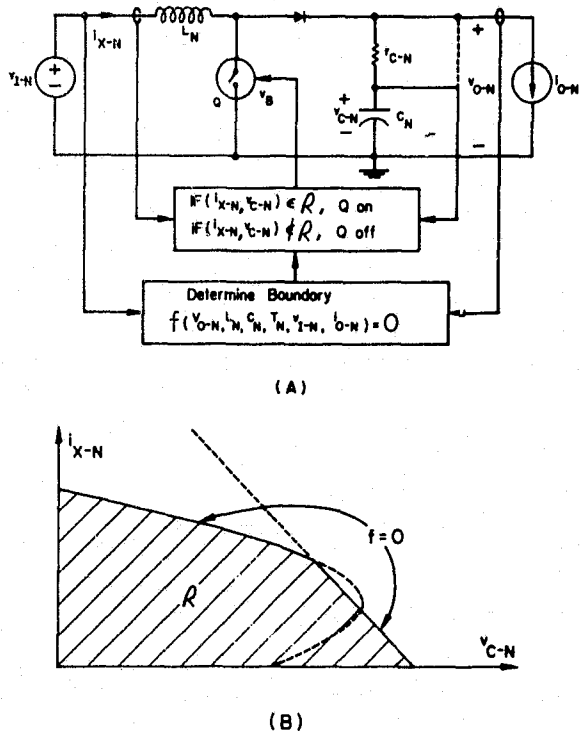

(A)

(B)

Fig. 18. (A) Conceptual diagram of free-running controller for the voltage step-up converter. (B) Definition of the function f and region R.

instantaneous values of input voltage and output current are used to construct the two-segment switching line illustrated graphically in Fig. 18 (B) and functionally identified by the expression $f(V_{O-N}, L_N, C_N, T_N, v_{I-N}, i_{O-N}) = 0$. With this switching line establishing the boundary of region R, the controller determines whether or not the instantaneous state of the power-handling subnetwork is contained within that region and turns the transistor switch on or off accordingly. The exact form of the switching line equation is dependent on the particular network model used to describe the converter. The development of this equation is, in fact, the only aspect of this approach which is dependent on the system model chosen.

Another system variable required of this controller is the output capacitor voltage. As stated earlier, the ideal capacitor voltage is not physically obtainable and thus the actual output voltage
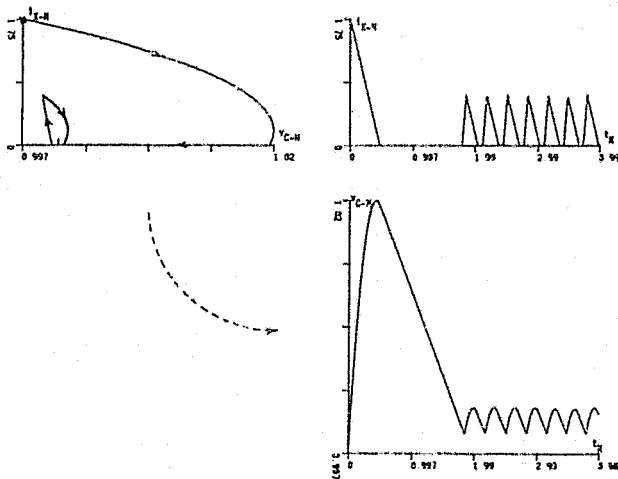
Fig. 19. CSMP generated response of the free-running converter system for a step decrease in I_{O-N} from 1.0 to 0.2.

Fig. 20. CSMP generated response of the free-running converter system for a step increase in I_{O-N} from 1.0 to 2.0.

is shown as an alternative input to the control process. In the latter case, the function f must be modified accordingly to yield an f' which is also a function of the capacitor ESR. The CSMP simulation data presented later in this section uses the output voltage as a controller input rather than the ideal capacitor voltage.

   As discussed in an earlier section, the shapes of the system on-time and off-time trajectories change when either the system parameters or operating conditions change. Fig. 17 illustrates the trajectories and the switching lines for the example converter operating under three different load conditions. If the system is operating in steady state at 100% of the rated output current, the system state follows the closed trajectory at the center of Fig. 17(B). If the load current is suddenly reduced to 20% of the rated value, the trajectories plotted in Fig. 17(C) subsequently must be followed, and the bold switching line shown there should then be used. Similarly, if the load current is suddenly increased to 200% of its rated value, the trajectories and switching line drawn in Fig. 17(A) must then be followed.

   Computer simulations of these two transient responses are presented in Figs. 19 and 20. These cases are exactly the same as those illustrated in Figs. 12, 13, 15, and 16 except that now the system is operating under the control of the free-running controller outlined in this section. The initial state is the same as used previously and corresponds to the steady-state switch-off state for the example illustrated in Fig. 17(B). The CSMP generated plots are not to the same scale as the plots in Fig. 17, but one can mentally superimpose the transient trajectory displayed in Fig. 19 onto the plane of Fig. 17(C) to see how the system state moves from its initial state under one set of operating conditions to another steady-state trajectory under different operating conditions in one on/off cycle of control. Similarly, one can superimpose the transient trajectory of Fig. 20 onto the plane of Fig.
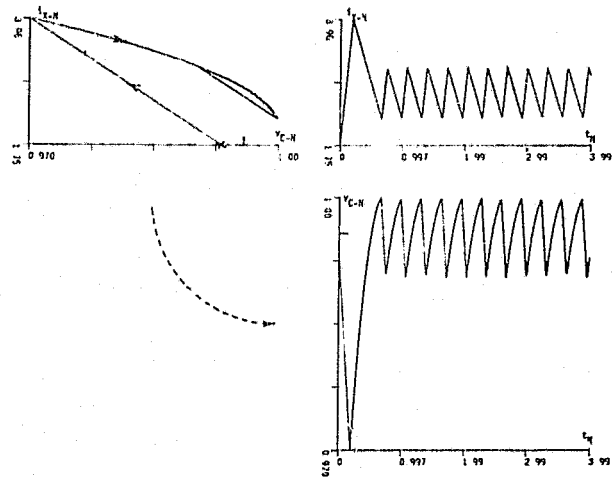
17(A) to see how steady-state operation is achieved at a heavier load condition, again in one on/off cycle of control. The accompanying time waveforms in Figs. 19 and 20 illustrate clearly the free-running nature of the converter during the initial on/off transient cycle and the constant frequency nature during steady-state operation, regardless of the system's initial state or the load conditions in effect.

   This same free-running control technique responds equally well to step-changes in input voltage. Fig. 5 presents the CSMP generated transient response of the example converter to an input voltage jump from 50% to 75% of the rated output voltage. Again the transition to the new steady-state condition is seen to be completed in one on/off switching cycle.

CONCLUSIONS

   A general, qualitative investigation of the voltage step-up dc-to-dc converter has been presented. The state-plane analysis approach employed in this investigation reveals families of trajectories which the converter state must follow during transistor on-time and off-time as a result of the system's governing physical laws. An understanding of these trajectories and knowing how they change for changes in system parameters and externally imposed operating conditions reveal certain fundamental limitations in the performance of the converter power stage which cannot be exceeded no matter what control technique is employed. This ability to observe the movement of the system state enables one to examine and compare various control techniques which can be used to determine when to switch the converter power transistor on and off and to determine strengths and weaknesses in these techniques. Furthermore, by using the information which is contained in these state trajectories, a control law for a free-running voltage step-up converter has been conceptually developed which can move the converter state from

any initial condition to steady-state operation in one on/off cycle of control. A converter running under the control of this law can respond equally well to changes in input voltage and changes in output current. Circuit protection features, such as current or voltage limiters, can also be included in such a controller, with the system state trajectories again revealing the precise manner in which these desired features can be achieved.

The principal function of energy-storage dc-to-dc power converters is to extract electrical energy from a given source at some unregulated voltage level, but at a controlled rate, in order to deliver energy to an electrical load at a different specified voltage level and particular power level. The only means available for controlling this rate of energy extraction is the switching on and off of the converter power transistor, which is of course the principal task of any controller. With such an a priori limitation in the ability to continuously control this flow of energy, further restrictions imposed on the control process such as fixing the transistor on-time or, even more restrictive, fixing the converter switching frequency can only cause degradation from the theoretically achievable converter performance. Thus, only by utilizing all of the information available from the system, and by allowing the transistor switch to remain on and off for variable time periods can the theoretical limits in converter performance be approached. Such a free-running converter which adapts to changes in system operating conditions is proposed herein. While providing superior performance, this approach also requires considerably more complex circuitry to implement than the more conventional control techniques in widespread use today. Thus, as is often the case, the system designer and user must trade-off the complex circuitry and resultant decrease in system reliability against the desired improved converter performance.

All of the discussions and the free-running control law presented in this paper have been illustrated through application to a voltage step-up energy storage dc-to-dc converter. Nothing in the development of this approach is dependent on this particular choice for an example system, however, and it is therefore belived that this approach and control technique are equally applicable to the other commonly used configurations for energy storage dc-to-dc converters.

REFERENCES

1. B. P. Schweitzer and A.B. Rosenstein, "Free Running - Switching Mode Power Regulator: Analysis and Design," IEEE Transactions on Aerospace and Electronic Systems, Vol. AS-2, pp. 1171-1180, October 1964.

2. I.M.H. Babaa, T.G. Wilson, and Y. Yu, "Analytic Solutions of Limit Cycles in a Feedback- Regulation Converter System with Hysteresis," IEEE Transactions on Automatic Control, Vol. AC-13, No. 5, pp. 524-531, October 1968.

3. F.F. Judd and C.T. Chen, "Analysis and Optimal Design of Self-Oscillating DC-to-DC Converters," IEEE Transactions on Circuit Theory, Vol. CT-18, No. 6, pp. 651-685, November 1971.

4. G.W. Wester and R.D. Middlebrook, "Low-Frequency Characterization of Switched dc-dc Converters," IEEE Transactions on Aerospace and Electronic Systems, Vol. AES-9, No. 3, pp. 376-385, May 1973.

5. F.C. Schwarz, "Engineering Information on an Analog Signal to Discrete Time Interval Converter (ASDTIC)," NASA CR- 134544, June 1974.

6. A.K. Ohri, H.A. Owen, Jr., T.G. Wilson, and G.E. Rodriguez, "Digital Computer Simulation of Inductor-Energy-Storage DC-to-DC Converters with Closed-Loop Regulators," S.P. 103, ESRO Spacecraft Power Conditioning Electronics Seminar, Frascati, Italy, May 1974.

7. A. Capel, J.G. Ferrante, and R. Prajoux, "State Variable Stability Analysis of Multi-Loop PWM Controlled DC/DC Regulators in Light and Heavy Mode," IEEE Power Electronics Specialist Conference Record, pp.91-102, June 1975.

8. P. Burger, "Analysis of a Class of Pulse Modulated DC-to-DC Power Converters," IEEE Transactions on Industrial Electronics and Control Instrumentation, Vol. IECI-22, No. 2, pp. 104-116, May 1975.

9. R.P. Iwens, Y. Yu, and J.E. Triner, "Time Domain Modelling and Stability Analysis of an Integral Pulse Frequency Modulated DC to DC Power Converter," IEEE Power Electronics Specialists Conference Record, pp.80-90, June 1975.

10. R. Prajoux, A. Giraud, and R. Valette, "A Modeling Technique Using A Recurrence for Some Control Systems Described by a Piecewise-Time-Invariant-Continuous State Equation," Conference on Information Sciences and Systems, The John Hopkins University, Baltimore, Md., April 2-4, 1975.

11. J. Jalade, "Contribution à l'Étude des Systèms Nonlinéaires à Structure Linéaire par Morceaux: Application à l'Étude par un Modèle Discret des Convertisseurs Continu-Continu, "Doctoral Thesis, University Paul Sabatier, Toulouse, France, 1976.

12. J.C. Marpinard, "Contribution à l'Étude des Systèmes Nonlinéaires à Structure Linéaire par Morceaux: Application à l'Étude par un Modèle de Type Continu des Convertisseurs Continu-Continu," Doctoral Thesis, University Paul Sabatier, Tousouse, France, 1976.

13. L.O. Chua, Introduction to Nonlinear Network Theory, Chap. 19. New York: McGraw-Hill, 1969.

14. D.Y. Chen, H.A. Owen, Jr., T.G. Wilson, "Energy-Balance Constraints Affecting the Design of Energy-Storage DC-to-DC Converters," IEEE 1975 Applied Magnetics Workshop, IEEE Publication 75CH0964-7MAG, pp. 3B-1 to 3B-22, June 1975.